

RESEARCH ARTICLE

The mayfly *Neocloeon triangulifer* senses decreasing oxygen availability (P_{O_2}) and responds by reducing ion uptake and altering gene expression

Jamie K. Cochran and David B. Buchwalter*

ABSTRACT

Oxygen availability is central to the energetic budget of aquatic animals and may vary naturally and/or in response to anthropogenic activities. Yet, we know little about how oxygen availability is linked to fundamental processes such as ion transport in aquatic insects. We hypothesized and observed that ion (^{22}Na and $^{35}\text{SO}_4$) uptake would be significantly decreased at O_2 partial pressures below the mean critical level (P_{crit} , 5.4 kPa) where metabolic rate (\dot{M}_{O_2}) is compromised and ATP production is limited. However, we were surprised to observe marked reductions in ion uptake at oxygen partial pressures well above P_{crit} , where \dot{M}_{O_2} was stable. For example, SO_4 uptake decreased by 51% at 11.7 kPa and 82% at P_{crit} (5.4 kPa) while Na uptake decreased by 19% at 11.7 kPa and 60% at P_{crit} . Nymphs held for longer time periods at reduced P_{O_2} exhibited stronger reductions in ion uptake rates. Fluids from whole-body homogenates exhibited a 29% decrease in osmolality in the most hypoxic condition. The differential expression of *atypical guanylate cyclase* (*gcy-88e*) in response to changing P_{O_2} conditions provides evidence for its potential role as an oxygen sensor. Several ion transport genes (e.g. *chloride channel* and *sodium-potassium ATPase*) and hypoxia-associated genes (e.g. *ldh* and *egl-9*) were also impacted by decreased oxygen availability. Together, the results of our work suggest that *N. triangulifer* can sense decreased oxygen availability and perhaps conserves energy accordingly, even when \dot{M}_{O_2} is not impacted.

KEY WORDS: Osmoregulation, Oxygen sensing, Hypoxia, P_{crit} , Gene expression

INTRODUCTION

Dissolved oxygen (DO) is an important abiotic factor that varies naturally and plays roles in the distribution of aquatic species (Blaszcak et al., 2019; Eriksen, 1968; Hoback and Stanley, 2001; Huryn and Wallace, 2000). Hypoxia can occur naturally, most frequently at night when photosynthesis cannot counteract respiration, in stagnant waters and in areas with abundant organic matter or impeded flow (Resh et al., 2008). Anthropogenic activities exacerbate this and have led to growing concerns about hypoxia,

globally. Nutrient runoff, eutrophication and changing global temperatures can all lead to hypoxic events (Diaz, 2001; Friedrich et al., 2014; Jenny et al., 2016a,b; Meire et al., 2013; Nixon, 1995). Hypoxia has the potential to impact all but the most hypoxia-tolerant aquatic species. Aquatic insects play disproportionately significant roles in these ecosystems and are widely used in ecological monitoring programs to make inferences about ecological conditions (Funk et al., 2006; Hawkins, 2006; Hawkins et al., 2000; Resh and Jackson, 1993). Oxygen availability is central to the energetic budget of these aquatic animals, and a lack of available DO can cause a cascade of effects.

Many organisms maintain a stable rate of oxygen consumption (\dot{M}_{O_2}) until they reach a point where their \dot{M}_{O_2} becomes dependent on the amount of available oxygen (Brodersen et al., 2008; Lencioni et al., 2008; Pörtner and Grieshaber, 1993). The environmental oxygen level (P_{O_2}) where an organism can no longer oxyregulate is traditionally called the P_{crit} . While P_{crit} has been questioned as an indicator of hypoxia tolerance (Wood, 2018), it clearly has importance to the organism. For example, in the mayfly *Neocloeon triangulifer*, P_{crit} has been associated with significant upregulation of the hypoxia-responsive genes *egl-9* (egg laying deficient, an oxygen-sensing gene and modulator of HIF-1a activity) and *ldh* (lactate dehydrogenase, a hypoxia indicator) (Cochran et al., 2021). This suggests that P_{crit} represents a shift from aerobic to anaerobic metabolism in this species. As sufficient oxygen is necessary to convert nutrients into ATP, decreasing P_{O_2} results in decreased ATP synthesis, leading to a cascade of effects including decreased energy production, greater reliance on anaerobic respiration, and reallocation of energy to increase ventilation (Boutilier and St-Pierre, 2000; Verberk et al., 2020), specifically at P_{O_2} below P_{crit} . As a result, aquatic insects (like other animals) must prioritize or allocate their energy expenditure. It is currently unknown where osmoregulation falls in terms of their energy prioritization.

Osmoregulation in freshwater is considered energetically expensive but physiologically crucial. Freshwater environments are typically strongly hypotonic to the organism's hemolymph, and therefore preventing excess ion loss and water uptake is critical in maintaining homeostasis (Silver and Donini, 2021). When ATP turnover is decreased in environments with decreased oxygen, it is unknown exactly how osmoregulatory function is impacted in aquatic insects. Studies in freshwater fish have found reduced sodium and water fluxes after exposure to severe hypoxia, with some differences existing between hypoxia-tolerant and less tolerant taxa (Giacomin et al., 2020; Iftikar et al., 2010; Onukwufor and Wood, 2020, 2018; Robertson et al., 2015; Wood et al., 2019, 2009, 2007; Wood and Eom, 2021). However, we are unaware of any studies that address osmoregulatory changes in freshwater insects, specifically at environmental oxygen levels that are reduced, but not low enough to cause physiological hypoxia.

Department of Biological Sciences, North Carolina State University, Raleigh, NC 27695, USA.

*Author for correspondence (david_buchwalter@ncsu.edu)

ID J.K.C., 0000-0002-2915-9408; D.B.B., 0000-0002-4372-1268

This is an Open Access article distributed under the terms of the Creative Commons Attribution License (<https://creativecommons.org/licenses/by/4.0>), which permits unrestricted use, distribution and reproduction in any medium provided that the original work is properly attributed.

Received 19 April 2024; Accepted 8 October 2024

Animals have evolved mechanisms to sense O_2 concentration, with studies in large vertebrates revealing sophisticated neuronal circulatory and respiratory systems (Ma and Ringstad, 2012). However, little is known about similar systems in small invertebrates, such as aquatic insects. Studies in the nematode *Caenorhabditis elegans*, the fly *Drosophila melanogaster* and the crustacean *Procambarus clarkii* have identified guanylate cyclase (GC) subunits (e.g. *gcy-88e*) and hypoxia-inducible transcription factors (HIFs) as O_2 -sensing molecules (De Lima et al., 2021; Ma and Ringstad, 2012). The oxygen-sensing prolyl hydroxylase *egl-9* (also referred to as *hph* and *phd*) hydroxylates HIF to tag it for destruction, thereby abolishing signaling activity under normal conditions. Under hypoxic conditions, *egl-9* cannot hydroxylate HIF, which results in the accumulation of HIF and *egl-9* (Bishop et al., 2004; Cochran et al., 2021; Kim et al., 2017; Ma and Ringstad, 2012; Semenza, 2001; Shao et al., 2009; Shen and Powell-Coffman, 2003). In the mayfly *N. triangulifer*, measurement of HIF1 α mRNA expression suggests it is constitutively expressed, with *egl-9* controlling HIF1 α activity (K. S. Kim and D.B.B., unpublished data). However, to our knowledge there have been no other studies on oxygen sensing in aquatic insects to date.

Here, we used the lab-reared mayfly *N. triangulifer*, a parthenogenic species emerging as a useful model for ecological (Sweeney and Vannote, 1984), toxicological (Conley et al., 2014; Johnson et al., 2015; Kunz et al., 2013; Soucek and Dickinson, 2015; Sweeney et al., 1993; Xie and Buchwalter, 2011) and physiological studies (Chou et al., 2018; Cochran et al., 2021; Cochran and Buchwalter, 2022; Kim et al., 2017; Orr et al., 2021). Specifically, we exposed nymphs to ramps of dissolved oxygen, using P_{crit} estimates for *N. triangulifer* at 22°C (Cochran et al., 2021) to inform P_{O_2} set points. We used a radiotracer approach to ask whether Na and SO₄ uptake rates were impacted by decreased oxygen availability (ranging from normoxia to hypoxia). We also measured the osmolality of fluids from whole-body homogenates and assessed the mRNA expression levels of hypoxia-responsive genes (*egl-9* and *ldh*) and genes related to ion transport (Orr et al., 2021) across the same environmental oxygen levels. Finally, we capitalized on our newly annotated *N. triangulifer* genome (NCBI GCF_031216515.1) to develop a qPCR probe for the oxygen-sensing *gcy-88e* gene.

MATERIALS AND METHODS

Animal collection and rearing

Neocloeon triangulifer (WCC-2 clone) were originally obtained from White Clay Creek in Pennsylvania by collaborators at Stroud Water Research Center (SWRC; Avondale, PA, USA) (Sweeney and Vannote, 1984). Nymphs were reared at North Carolina State University in 4-quart (~4 l) glass Pyrex dishes filled with Artificial Soft Water (ASW) and lined with WCC periphyton plates at room temperature with gentle aeration, and a 14 h:10 h light:dark photoperiod. ASW was made with recipes from the United States Environmental Protection Agency (D. Mount, EPA, Duluth, MN, USA, 2017, personal communication) using a base of distilled water (~17.8 MΩ) and laboratory-grade salts (Thermo Fisher Scientific, Waltham, MA, USA). Major ion concentrations of ASW (mg l⁻¹) were determined to be: 27.5 Na, 15.5 S, 6.0 Ca, 2.2 Mg, 2.2 K by ICP-MS at NCSU's EATS laboratory. Mature nymphs (~25 day rearing) were then removed from rearing dishes and used in experiments.

Controlled oxygen experiments

The overall design of this experiment was to 'step down' larvae from normoxia (21 kPa) to progressively lower P_{O_2} (11.7, 8.5, 5.4 and 1.6 kPa), and measure changes in ion transport rates and the

expression of a suite of genes related to oxygen sensing and ion transport. These methods and procedures to compare the responses of nymphs that had been stepped down sequentially with the responses of 'naive' nymphs that had previously been exposed to only 21 kPa are described in detail below. The P_{O_2} treatments were based in part on a previous study (Cochran et al., 2021) that characterized population mean, maximum and minimum P_{crit} estimates in this species.

To achieve the desired P_{O_2} treatments, tanks of compressed nitrogen (Arc3® gases UN1066; Fisherbrand™ Single-Stage Pressure Regulator with SCFH air flow meter) and compressed breathing quality air (Arc3® gases UN1002; Harris® model 425-125 Premium Single-Stage Pressure Regulator with SCFH air flow meter) were attached to a gas mixer, which distributed mixed air into a distribution manifold. Tubing from the manifold attached to 20 ml glass Wheaton® liquid scintillation vials through lids with drilled bore holes to accommodate 1000 µl Fisherbrand™ Redi-Tip™ pipette tips and a smaller vent hole were used to control gas exchange with the room. Four of the 11 total chambers were used to monitor the experimental oxygen tension throughout the 15 h experiment (Fig. 1), with calibrated oxygen sensor spots and AutoResp™ software. Two of these monitoring chambers contained only water and two contained nymphs to ensure that their presence did not significantly alter the intended oxygen tensions in unmonitored experimental vials. Including the two monitored chambers, there were 9 total 'experimental' chambers that contained nymphs (see Figs S1 and S2 and Table S1 for a full overview). The vials contained 10 ml of ASW and were kept on the benchtop at room temperature. Temperature was constantly monitored using the AutoResp™ software in a separate vial kept on the benchtop. See Fig. S1 for setup.

Between 10 and 19 individuals were introduced into each of the 9 experimental vials (Fig. 1A) at the beginning of the experiment and exposed to 21 kPa for 3 h. A subset of animals (2–4 per vial) were collected after the 3 h exposure to 21 kPa (Fig. 1B) as controls. Eight individuals (from waters containing radioisotope) were collected for ion flux experiments (see 'Ion flux' section below for specific procedure), 5 were collected for osmolality measurements (see 'Osmolality' section below for specific procedure) and 10 were collected for gene expression (see 'Gene expression' section below

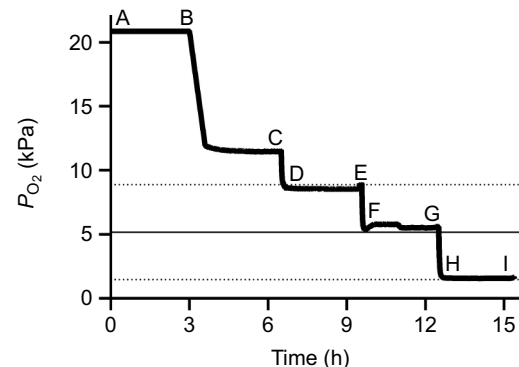


Fig. 1. Oxygen partial pressure (P_{O_2}) and *Neocloeon triangulifer* nymph sampling points at 22°C. Each letter denotes when nymphs were sampled for ion flux, osmolality and gene expression studies (as described in Materials and Methods, see Table S1). Letters D, F and H denote when a new cohort of naive nymphs was added to each exposure for a subset of the ion flux data. Dashed lines represent maximum and minimum critical oxygen partial pressure (P_{crit}) estimates and the solid line represents mean P_{crit} from Cochran et al. (2021).

for specific procedure). The remaining individuals were then ‘stepped down’ to 11.7 kPa and a similar subset of animals was collected from each vial at the end of the 3 h exposure period (Fig. 1C).

P_{O_2} was then decreased again to 8.5 kPa. To compare the responses of larvae that had experienced the previous P_{O_2} drops with those of larvae that had only previously experienced normoxic waters, 10 normoxic individuals were added to one vial containing 10 ml of non-radioactive ASW and 8 individuals were added to the last vial containing 10 ml of radioactive ASW. This group of individuals was exposed instantaneously to a given P_{O_2} and did not experience any prior decreased oxygen regimes (Fig. 1D). These individuals were only used for a subset of the ion flux data (Fig. 2).

After a 3 h exposure to 8.5 kPa, a similar subset of individuals was collected from the vials of individuals exposed to all prior P_{O_2} (2–4 per vial). From the newly introduced vials of naive individuals, all 8 of the nymphs were removed (Fig. 1E).

P_{O_2} was then decreased again, this time to 5.4 kPa, and the same methodology was used. Eight naive individuals were introduced into the radioactive empty vial (Fig. 1F). After a 3 h exposure to 5.4 kPa, the same number of individuals was collected from all vials (Fig. 1G).

P_{O_2} was then decreased again, to 1.6 kPa, and the same methodology was used. Eight naive individuals were introduced into the radioactive empty vial (Fig. 1H). After a 3 h exposure to 1.6 kPa, all individuals were collected from all vials (Fig. 1I).

Ion flux

Dual-labeled radioactive experimental waters were made by spiking $^{22}\text{NaCl}$ and $\text{Na}_2^{35}\text{SO}_4$ (PerkinElmer, Billerica, MA, USA) into ASW to achieve exposure activities of 150–215 Bq ml $^{-1}$. Exposures were measured with a Beckman LS6500 Multipurpose Scintillation Counter (Beckman Coulter, Brea, CA, USA) immediately before the experiments began.

Eight nymphs were removed from the radioactive exposure waters by gently pipetting them into a mesh strainer (collecting any residual radioactive water in a waste container) and gently blotting them dry. The nymphs were then rinsed in two consecutive water baths of ASW to remove loosely adsorbed ions from the exoskeleton. After rinsing, nymphs were blotted dry, weighed, and digested in 500 μl of Soluene 350 (PerkinElmer) in a 20 ml glass vial at 28°C. After 48 h, they were neutralized with 500 μl of glacial acetic acid and 12 ml of scintillation cocktail (PerkinElmer Ultima Gold uLLT).

Uptake rates were calculated as the slopes of linear regressions of time on mass of ion (Na or SO_4) accumulated per gram bug mass (GraphPad Prism v9.4.0, GraphPad Software, La Jolla, CA, USA). Mass-specific calculations were based on wet mass. We applied appropriate corrections for spill-over and quench, and only measurements with lumex values <5% and error rates <10% were used in analyses. Linear regressions were performed to analyze the relationship between treatment and ion flux rates using GraphPad Prism (v9.4.0, GraphPad Software).

Osmolality

Five *N. triangulifer* nymphs were collected, blotted dry and weighed, then placed in a 1.5 ml microcentrifuge tube, flash frozen and kept in a –80°C freezer for 1 week. Samples were then homogenized. Briefly 30 μl of deionized water was added to the microcentrifuge tube, then samples were crushed with a plastic micropellet. After being briefly (~3 min) heated in a 70°C water bath, samples were spun in a centrifuge for 10 min. The supernatant

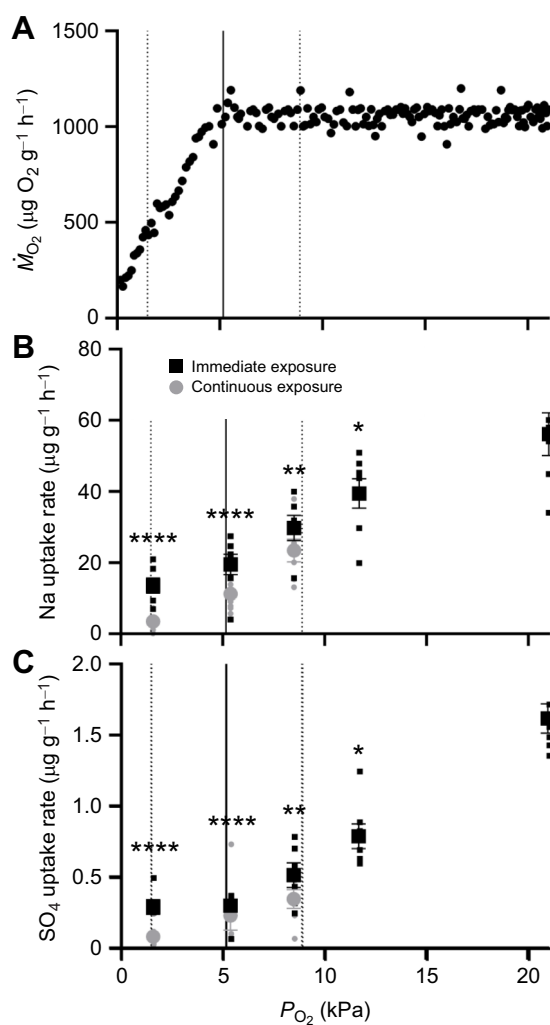


Fig. 2. *Neocloeon triangulifer* ion flux rates at different P_{O_2} . (A) Representative metabolic rate (M_{O_2}) against P_{O_2} for one *N. triangulifer* individual from Cochran et al. (2021). Dashed lines represent maximum and minimum P_{crit} estimates, and the solid line represents mean P_{crit} estimated from 31 individuals at 22°C from Cochran et al. (2021). (B) Na and (C) SO_4 uptake rates of *N. triangulifer* in depleted oxygen partial pressures (21–1.6 kPa) at 22°C (mean±s.e.m., $n=7$ –8). Black squares represent nymphs that were introduced into chambers after the P_{O_2} was achieved, while gray circles represent nymphs that were introduced at the beginning of the experiment and experienced all prior P_{O_2} levels. Differences among treatments were assessed using a one-way ANOVA and Tukey’s multiple comparisons test. All treatments were compared with the control (21 kPa) group. Asterisks represent significant differences compared with 21 kPa (* $P\leq 0.05$; ** $P\leq 0.01$; *** $P\leq 0.0001$).

was then transferred to a fresh microcentrifuge tube. Osmolality of each sample was measured in duplicate 10 μl aliquots of supernatant using a VAPRO® vapor pressure osmometer (Wescor®, Logan, UT, USA), calibrated with 100 and 290 mmol kg $^{-1}$ standards. Data were given in mmol kg $^{-1}$, then corrected to account for the measured osmolality of dilution water and sample mass. A one-way ANOVA followed by Tukey’s multiple comparisons test was used to test whether any differences in osmolality occurred between treatments (GraphPad Prism v9.4.0, GraphPad Software).

Gene expression

Gene expression at the whole-organism level was assessed by placing nymphs into sterile microcentrifuge tubes and immediately

flash freezing them in liquid nitrogen. Five replicates of two individuals were taken at each sampling point (21, 11.7, 8.5, 5.4 and 1.6 kPa). We used two genes previously shown to be responsive to physiological hypoxia in this species, *egl-9* and *ldh* (Chou et al., 2018; Kim et al., 2017), the oxygen sensing gene *gcy-88e*, as well as 9 other genes associated with osmoregulation (see Table 1). *Tubulin* (*tub*) was used as a housekeeping gene for reference (Table 1). Primers were verified through NCBI BLAST to ensure high similarity (>90%) between other more established species (e.g. *A. aegypti*, *D. melanogaster*) and the newly annotated *N. triangulifer* genome. Total RNA was isolated from each replicate using the SV Total RNA Isolation System (Promega, Madison, WI, USA) according to the manufacturer's protocol and quantified on a NanoDrop™ 1000 (Thermo Fisher Scientific, Waltham, MA, USA). Then, first-strand cDNA was synthesized from 1 µg of RNA from each sample by MultiScribe™ MuLV reverse transcriptase using random primers (Applied Biosystems, Carlsbad, CA, USA) in 20 µl reactions using a Bio-Rad iCycler (Bio-Rad, Hercules, CA, USA). qPCR was performed on a QuantStudio™ 3 (Thermo Fisher Scientific) using SYBR® Green Supermix (Bio-Rad) in 10 µl reactions with technical triplicates. Custom parameters were used: 2 min at 50°C, 10 min at 95°C, followed by 40 cycles of 95°C for 15 s and 60°C for 1 min. Finally, a melt curve was calculated for each well to ensure sufficient quality of the samples. The delta CT method (Pfaffl, 2001) was used to analyze the relative expression of each amplicon. Expression levels of *tub* were approximately equal across all treatments and were used to normalize results. Primer efficiencies were included in the calculations to normalize expression. Differences among treatments in gene expression were assessed using a one-way ANOVA and Tukey's multiple comparisons test. All treatments were compared with the control (21 kPa) group to quantify differences of gene expression, unless otherwise stated.

RESULTS

Ion flux

There were no observed mortalities when nymphs were exposed to gradients in oxygen. \dot{M}_{O_2} decreased with lower P_{O_2} , with the P_{crit} occurring somewhere between 1.6 and 8.5 kPa for all 31 individuals at 22°C in Cochran et al. (2021) (Fig. 2A). Na uptake rates (Fig. 2B) and SO_4 uptake rates (Fig. 2C) were reduced in treatments below 11.7 kPa. At 11.7 kPa, Na uptake was 19% decreased relative to that at 21 kPa ($P=0.0571$; Fig. 2B) and SO_4 uptake was decreased 51% ($P=0.0175$; Fig. 2C) relative to that at 21 kPa ($P=0.0128$; Fig. 2C). Individuals continuously exposed to all of the preceding conditions of this P_{O_2} ramp had marked reductions in their ion uptake rates relative to individuals that were immediately transferred to each condition at 8.5 kPa and below (gray circles versus black squares in Fig. 2B,C).

For individuals only in the experimental water for the 3 h exposure (immediately exposed) at 8.5 kPa, Na uptake was 39% decreased relative to that at 21 kPa ($P=0.0080$; Fig. 2B) and SO_4 uptake was 68% decreased relative to that at 21 kPa ($P=0.0077$; Fig. 2C). At 8.5 kPa, Na and SO_4 uptake in continuously exposed nymphs was 33% ($P=0.0024$; Fig. 2C) and 40% ($P=0.0020$; Fig. 2C) lower than uptake in immediately exposed nymphs, respectively. At 5.4 kPa, Na uptake was 60% decreased relative to that at 21 kPa ($P<0.0001$; Fig. 2B) and SO_4 uptake was 82% decreased relative to that at 21 kPa ($P<0.0001$; Fig. 2C) for immediately exposed nymphs. Na and SO_4 uptake in continuously exposed nymphs was 62% ($P<0.0001$; Fig. 2B) and 66% ($P<0.0001$; Fig. 2C) lower than uptake in immediately exposed nymphs, respectively. At 1.6 kPa, Na uptake was 72% decreased relative to that at 21 kPa ($P<0.0001$; Fig. 2B) and SO_4 uptake was 82% decreased relative to that at 21 kPa ($P<0.0001$; Fig. 2C) for immediately exposed nymphs. At 1.6 kPa, Na and SO_4 uptake in continuously exposed nymphs was 75% ($P<0.0001$; Fig. 2B) and 93% ($P<0.0001$; Fig. 2C) lower than uptake in immediately exposed nymphs, respectively.

Table 1. Gene names, accession numbers, amplicon size and forward/reverse sequences for primers used in qPCR analysis

Gene name	Abbreviation/symbol	Accession no.	Primer efficiency	Amplicon	Oligonucleotide sequence (5' to 3')
<i>tubulin</i>	<i>tub</i>	MF463012	94	219	F: ATG CCC TCT GAC AAG ACT GTT GGA R: ATA GTG ACC GCG AGC GTA GTT GTT
<i>egg laying deficient 9</i>	<i>egl-9</i>	JF697592	114	244	F: CTG ACC AGG AAC GAC CTG AAG AC R: TGT TCG GAT TGT CCA CGT GCT TC
<i>lactate dehydrogenase</i>	<i>ldh</i>	JX675218	72	214	F: ACA CAA CGC TTC CTG TTT GGT CTG R: TTT CTG AGA ATG GTC TGC ACC AGG
<i>guanylate cyclase 88e</i>	<i>gcy-88e</i>	NW26775556	88	232	F: CCG AGT ACG TCT GCA ATA TG R: CAC ACT CGC CTC GAT TAT AC
<i>sulfate transporter</i>	<i>st</i>	MH549240	60	204	F: TGA TCA TTA CCG GCA TCA TCG GCT R: TTT CCA GAA TGG CGA GGA TAG GCA
<i>sodium-independent sulfate transporter</i>	<i>sist</i>	MH549239	95	181	F: CTT CAT TCC ACG CAC TAC C R: CAC CAC CAT GCC GAT TAG
<i>sodium bicarbonate cotransporter</i>	<i>sbc</i>	EFN72923	99	198	F: AGG CGA TCT GCT GCT GAG AAG AAT R: GAC TTG TTT CCA AAC GCC GCT CTT
<i>sodium-potassium ATPase</i>	<i>spa</i>	MF463013	82	234	F: CAG GCA CCA CAC TGA AAT R: GTG ACG ATG GAG GCA AAG
<i>calcium-transporting ATPase</i>	<i>cta</i>	MF463016	85	217	F: TTA CCC TCT CTC TGG CTT AC R: TCC ACT TCA GGA GGG ATG
<i>V-Type H⁺ ATPase</i>	<i>vha</i>	XP001845000	63	214	F: GCA CAA CCG ACA GAT CTA C R: GAA CTC GAG GTA GAG CAA ATC
<i>carbonic anhydrase</i>	<i>cah</i>	MF463016	73	177	F: ACA TTT ACA CCG GCG ACG TCT ACT R: CAG GTC TGC GGT TTG GCA ATG AAA
<i>aquaporin</i>	<i>aqp</i>	XP002425393	202	201	F: CGC TCG ATT CTC TCG TTT CTC R: TGT GTG TGT GTG TGT CTG TC
<i>chloride-channel</i>	<i>clch</i>	MF463015	59	214	F: CCT TGG TGT CAT CCT TCT TT R: CCA GAC TTC AGG ACA AAC TT

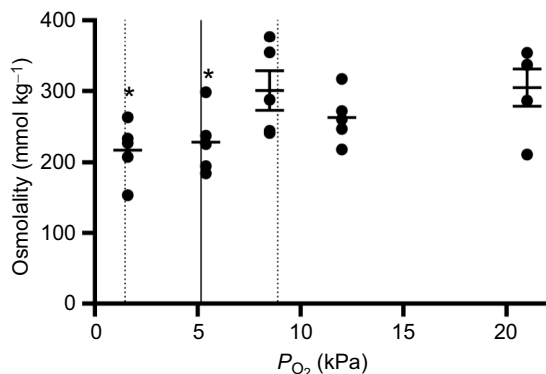


Fig. 3. *Neocloeon triangulifer* osmolality across a range of P_{O_2} (21–1.6 kPa). Data are means \pm s.e.m. ($n=5$). Dashed lines represent maximum and minimum P_{crit} estimates and the solid line represents mean P_{crit} from Cochran et al. (2021). Differences among treatments were assessed using a one-way ANOVA and Tukey's multiple comparisons test. All treatments were compared with the control (21 kPa) group. Asterisks represent significant differences compared with 21 kPa ($*P\leq 0.05$).

Osmolality

An unpaired *t*-test showed a significant decrease in osmolality at and below P_{crit} (5.4 and 1.6 kPa; $P=0.0361$ and $P=0.0244$, respectively; Fig. 3). At 5.4 kPa, the osmolality was 25% lower than at 21 kPa and at 1.6 kPa the osmolality was 29% lower relative to that at 21 kPa.

Gene expression

The mRNA levels of nymphs at oxygen saturations above P_{crit} were not different from those of control (21 kPa) animals for *ldh* and *egl-9*. However, in the most hypoxic condition, nymphs had elevated expression for *ldh* (1.6 kPa, $P=0.03$; Fig. 4A) and *egl-9* (1.6 kPa, $P=0.007$; Fig. 4B).

At maximum and mean P_{crit} , nymphs had elevated expression of *gcy-88e* relative to control (21 kPa) animals (8.5 kPa, $P=0.04$; 5.4 kPa, $P=0.007$; Fig. 4C). Below P_{crit} , expression of *gcy-88e* was not statistically different from that of control animals (1.6 kPa, $P=0.4$; Fig. 4C).

Nymphs at oxygen saturations below control (21 kPa) varied in their mRNA levels of several other genes of interest. While some interesting trends in gene expression were observed, only *sodium-potassium ATPase* (*spa*) ($P=0.0002$; Fig. 5A), *sulfate transporter* (*st*) ($P<0.0001$; Fig. 5E), *sodium-independent sulfate transporter* (*sist*) ($P=0.0002$; Fig. 5F) and *chloride-channel* (*clch*) (8.5 kPa, $P=0.0103$; 5.4 kPa, $P=0.0012$; Fig. 5H) showed statistically significant upregulation with decreased P_{O_2} .

DISCUSSION

ATP turnover is reduced as animals are exposed to significant time in hypoxia and anoxia, leading to a cascade of effects including eventual cell death (Boutilier and St-Pierre, 2000). Therefore, we hypothesized that energetically expensive ion uptake would be suppressed when ATP production was suppressed, at partial pressures below P_{crit} . This is supported by previous studies looking into the osmorespiratory compromise (the trade-off between the demands of high gill permeability for respiration and low permeability for osmoregulation) in freshwater fish. Hypoxia-tolerant freshwater species such as the oscar (Wood et al., 2009, 2007), common killifish (Giacomin et al., 2020; Wood et al., 2019) and tambaqui (Robertson et al., 2015) reduce sodium and water fluxes within an hour of exposure to severe hypoxia, but recover

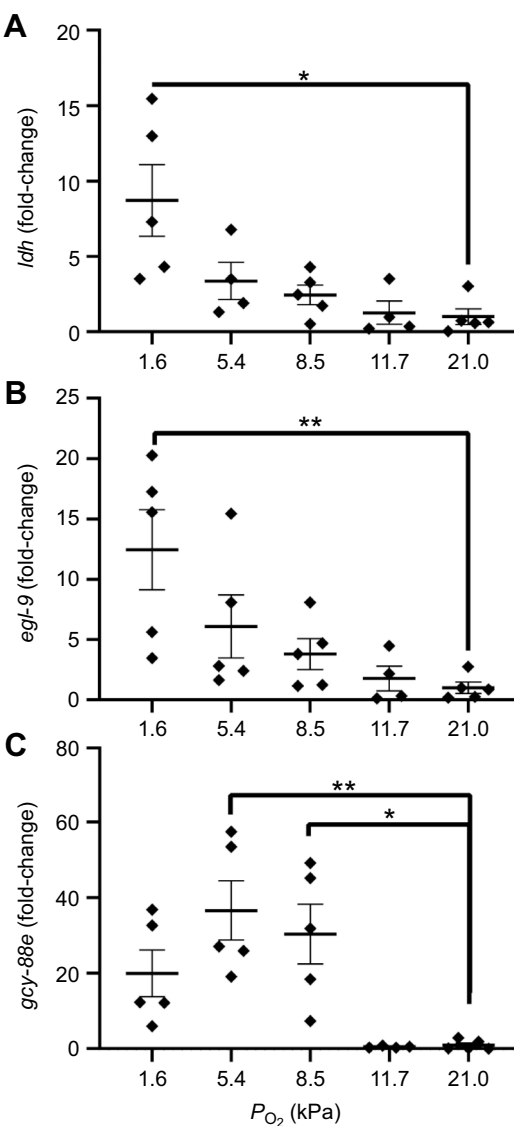


Fig. 4. Expression of hypoxia-associated genes in *N. triangulifer* across a range of P_{O_2} . Relative expression of (A) *ldh*, (B) *egl-9* and (C) *gcy-88e* after a 3 h exposure to different oxygen levels at 22°C. All data were normalized to expression of the housekeeping gene *tubulin*, and are expressed as fold-change relative to control samples (means \pm s.e.m., $n=5$ replicates of 2 individuals per replicate). Differences among treatments in gene expression were assessed using a one-way ANOVA and Tukey's multiple comparisons test. All treatments were compared with the control (21 kPa) group. Asterisks represent significant differences compared with 21 kPa ($*P\leq 0.05$; $**P\leq 0.01$).

within an hour of return to normoxia. Less hypoxia-tolerant species such as trout (Iftikar et al., 2010; Onukwufo and Wood, 2018) and zebrafish (Onukwufo and Wood, 2020) show elevated sodium and water fluxes at the start of acute hypoxia, but regulate both back towards control levels as hypoxia exposure continues and after return to normoxic conditions (Wood and Eom, 2021). However, in our study we observed significant impacts on uptake of both Na and SO₄ at partial pressures well above *N. triangulifer*'s P_{crit} at 22°C (Fig. 2). We posit that *N. triangulifer* could sense the modest decrease in P_{O_2} and therefore conserved energy by limiting ion turnover.

While we observed changes in ion uptake with immediate decreases in P_{O_2} , we only observed statistically significant changes

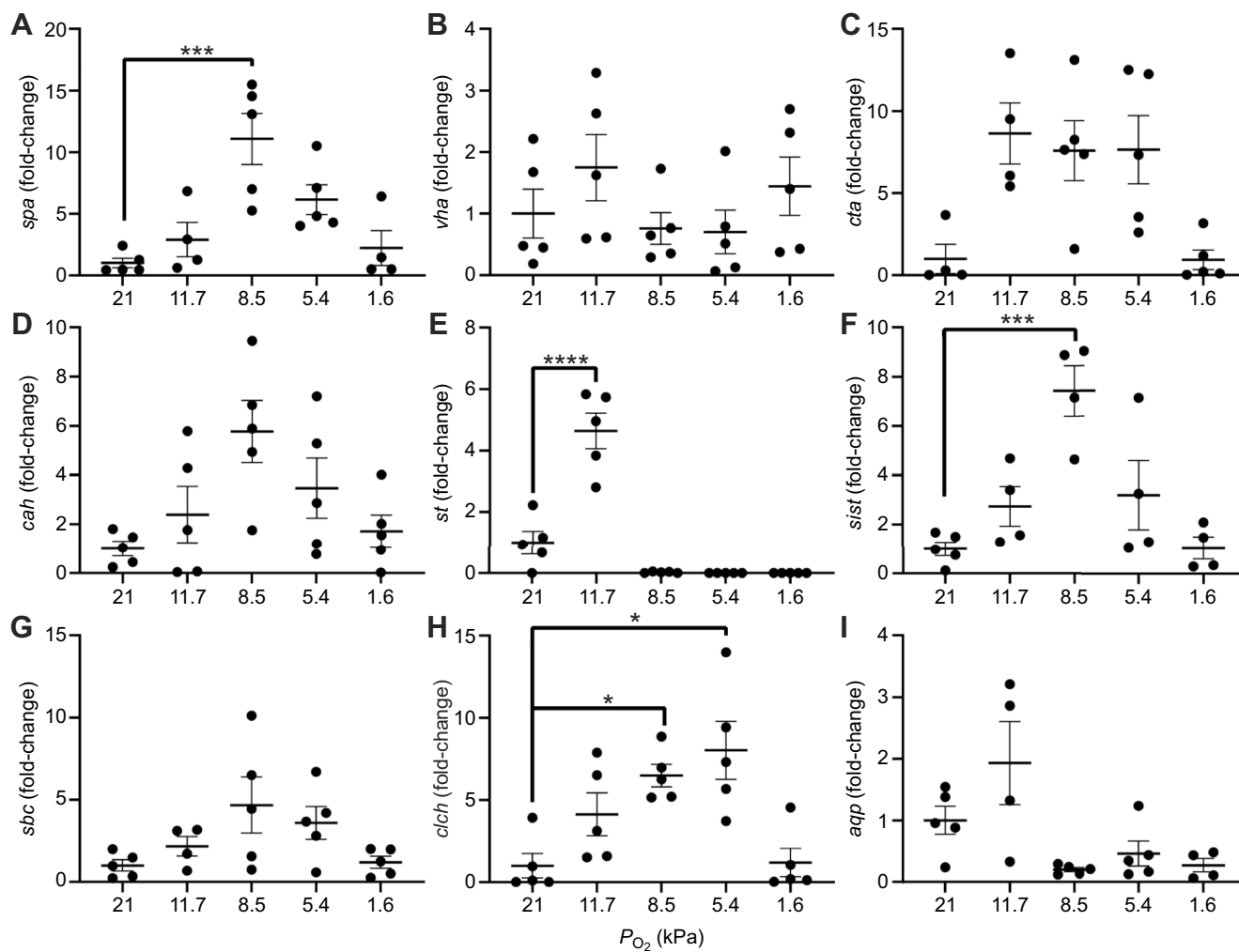


Fig. 5. Expression of ion transport genes in *N. triangulifer* across a range of P_{O_2} . Relative expression of (A) sodium-potassium ATPase (*spa*), (B) V-Type H^+ ATPase (*vha*), (C) calcium-transporting ATPase (*cta*), (D) carbonic anhydrase (*cah*), (E) sulfate transporter (*st*), (F) sodium-independent sulfate transporter (*sist*), (G) sodium bicarbonate cotransporter (*sbc*), (H) chloride-channel (*clch*) and (I) aquaporin (*aqp*) after a 3 h exposure to different oxygen levels at 22°C. All data were normalized to expression of the housekeeping gene *tubulin*, and are expressed as fold-change relative to control samples (means \pm s.e.m., $n=4$ –5 replicates of 2 individuals). Differences among treatments in gene expression were assessed using a one-way ANOVA and Tukey's multiple comparisons test. All treatments were compared with the control (21 kPa) group. Asterisks represent significant differences compared with 21 kPa (* $P\leq 0.05$; *** $P\leq 0.001$; **** $P\leq 0.0001$).

in osmolality at and below P_{crit} (Fig. 3). In previous studies in *N. triangulifer*, total body salts (Cochran and Buchwalter, 2022), sulfur (Buchwalter et al., 2019) and sodium (Scheibener et al., 2016) were strongly regulated despite changes in ion uptake rates. Our findings suggest that in individuals at and below P_{crit} , reduced ion uptake was at least transiently not offset by increased ion retention or reductions in diffusive ion loss (see Cochran et al., 2024). This could result in ionic dysregulation as a significant consequence of hypoxia in this species. Notably, with the osmolality measurements being from whole-body samples, there are limitations in the interpretation of this data. We suggest that more work is needed to understand whether ionic dysregulation is occurring during hypoxia in this species.

At the level of gene expression, we targeted several genes including some ion transporters and some hypoxia-responsive genes. Many important ion transporters and aquaporins have been identified to date in the mayfly *N. triangulifer*, and our group has previously found changes in *N. triangulifer* mRNA levels and specific proteins associated with salinity exposure (Orr et al., 2023, 2021). Despite seeing interesting trends in the

regulation of these genes across oxygen gradients (Table S2), statistically significant upregulation was only seen in *spa*, *st*, *sist* and *clch*.

Na^+/K^+ -ATPase maintains the ionic gradient across cell membranes and powers cellular functions. Decreases in mRNA expression with increased salinity have been observed in *N. triangulifer* (Orr et al., 2023). Here, *spa* showed gradual upregulation, with statistically significant upregulation occurring at 8.5 kPa, followed by downregulation at/below P_{crit} . Similar changes were observed in V-Type H^+ ATPase (*vha*), though this change was not statistically significant. V-type H^+ -ATPase functions as a proton pump to aid physiological function of cells (Finbow and Harrison, 1997) and has been linked to ion and water transport in aquatic insects (Nowghani et al., 2017; Weihrauch et al., 2001), with decreased expression in *N. triangulifer* with increased salinity (Orr et al., 2023). Jonusaite and colleagues (2013) found that ion reabsorption was significantly reduced when ion-motive pumps (V-type H^+ -ATPase and Na^+/K^+ -ATPase) were pharmacologically inhibited. These changes in the regulation of *vha* and *spa* suggest

that ion reabsorption may be inhibited at lower P_{O_2} and should be further studied.

The trend of immediate stimulation in upregulation with decreases in P_{O_2} followed by dramatic downregulation with continued exposure was also observed in *st*, with expression at 11.7 kPa being significantly increased ($P < 0.0001$, Fig. 5E). Sulfate transporters are not well understood to date, with some groups proposing that their function is to support reabsorption of essential ions (Markovich and Aronson, 2007) and other groups suggesting that they may be involved in efflux of excess major ions (Orr et al., 2023). We noted a gradual upregulation followed by downregulation at/below P_{crit} in *chloride-channel (clch)*, *sodium bicarbonate cotransporter (sbc)*, *sist* and *carbonic anhydrase (cah)*. However, only *clch* and *sist* showed statistically significant elevation.

It would be reasonable to expect that the observed decreases in ion uptake at lower oxygen partial pressures would be accompanied by decreased transporter expression. However, our findings seem to contradict this, with most transporters appearing to increase with lower P_{O_2} , as ion uptake decreases. We are unsure what led to this interesting finding. One possibility is that internally, ion-deficient tissues are upregulating their ion transport potential. Alternatively, these expression differences could represent the upregulation of transporters on the body surface if the nymphs were preparing themselves to increase transport if they were returned to normoxic conditions. Neither possibility can be substantiated however, and efforts are underway to examine gill-specific mRNA responses to hypoxia in isolated gills. Further, we posit that the observation of upregulation of expression of genes with initial decreases in oxygen and subsequent downregulation of expression with very low oxygen may be associated with upregulation of transcript abundance followed by translation into protein and subsequent depletion of mRNA as oxygen levels decline.

Interestingly, sustained O_2 -sensing signaling has been observed to rely on Ca^{2+} channel relays in *C. elegans* (Busch et al., 2012). Further, carbonic anhydrases are central in mammalian CO_2 detection and have been associated with CO_2 detection in fish gills (Hu et al., 2010; Scott, 2011; Tashian, 1989). Studies in *N. triangulifer* have observed differential regulation of these genes and gill proteome in response to salinity challenge (Orr et al., 2023, 2021), but to our knowledge no similar studies exist looking at upregulation of these genes in response to oxygen availability.

Two hypoxia-associated genes have previously been studied in relation to P_{crit} in *N. triangulifer*: *ldh* and *egl-9* (Cochran et al., 2021). Our results are commensurate with those of this previous study, with upregulation of both genes occurring below P_{crit} . Upregulation of *ldh* specifically suggests a switch from aerobic to anaerobic metabolism, which supports the notion that ATP production would be depleted after P_{crit} , and energetic constraints would be imposed. *egl-9* is an oxygen-sensing prolyl hydroxylase that turns off HIF signaling (Bishop et al., 2004; Epstein et al., 2001; Kim et al., 2017; Semenza, 2001; Shao et al., 2009; Shen and Powell-Coffman, 2003). Studies of the nematode *C. elegans*, the fly *D. melanogaster* and the crustacean *P. clarkii* have shown that HIF is an O_2 -sensing molecule that mediates the response to respiratory gases (De Lima et al., 2021; Ma and Ringstad, 2012). The upregulation of *ldh* and *egl-9* in our results suggest that this mechanism of O_2 sensing may be occurring below P_{crit} , but it does not explain the reduction in Na and SO_4 uptake rates at P_{O_2} above P_{crit} .

gcy-88e has also been identified as an oxygen-sensing gene in *C. elegans*, *D. melanogaster* and *P. clarkii* (De Lima et al., 2021; Ma and Ringstad, 2012). In *D. melanogaster*, the GC subunits

gcy-89da, *gcy-89db* and *gcy-88e* constitute a cyclase that directly binds to O_2 . After binding to O_2 , GCs can convert GTP to cyclic GMP (Ma and Ringstad, 2012). The recent annotation of the *N. triangulifer* genome (NCBI GCF_031216515.1) (O'Leary et al., 2016) allowed us to develop a gene-specific primer for *gcy-88e*. Our results show upregulation of *gcy-88e* at partial pressures approaching and below P_{crit} (though data below P_{crit} were not statistically significant). This is commensurate with the aforementioned observations and suggests that *N. triangulifer* is able to sense depleted oxygen prior to P_{crit} . Importantly, we only saw changes in *gcy-88e* expression at 8.5 kPa and below, but saw changes in ion transport and regulation of other genes (e.g. *clch*, *sbc*) prior to these P_{O_2} . We posit that there may be other oxygen sensing occurring to stimulate those changes prior to upregulation of *gcy-88e*, though we are unsure what those may be. Alternatively, *gcy-88e* may be activated independent of changes in gene expression, with gene expression increasing with delay but protein detecting changes in oxygen earlier on. While we are still uncertain where this sensing is occurring, insects have many chemoreceptors, thermoreceptors and mechanoreceptors which can appear as hairs, campaniform sensilla or chordotonal organs (Keil, 2012; Rebora et al., 2019). Many chemoreceptors have specifically been described in the antennae and gills (Rebora et al., 2019; Wichard et al., 1973).

A recent study of chronic oxygen limitation throughout development in *N. triangulifer* found that as DO decreases, survival, adult mass and instantaneous growth rate decrease while gill size increases (Funk et al., 2021). These changes suggest that the energy budgets for development, reproduction and growth may be reallocated to oxyregulation in limited oxygen environments. More work is needed to understand the chronic impacts of hypoxia on osmoregulation and possible subsequent physiological changes. Further work is also needed to identify the specific locations and mechanisms of oxygen (and salinity) sensing in aquatic insects. It would also be beneficial for future studies to query what other genes may be impacted by depleted oxygen. Questions also remain as to what P_{O_2} are associated with the onset of oxygen sensing, and whether *N. triangulifer* nymphs energetically prioritize osmoregulation again when returned to normoxic conditions. This work signifies a first step in elucidating how oxygen is sensed and responded to in *N. triangulifer* nymphs, even in oxygen conditions not associated with anaerobic metabolism.

Acknowledgements

We thank Bradley Taylor, Russell Borski and Charles Hawkins for providing helpful comments on the manuscript.

Competing interests

The authors declare no competing or financial interests.

Author contributions

Conceptualization: J.K.C., D.B.B.; Methodology: J.K.C., D.B.B.; Formal analysis: J.K.C.; Investigation: J.K.C.; Writing - original draft: J.K.C.; Writing - review & editing: D.B.B.; Funding acquisition: D.B.B.

Funding

This research was supported by the National Science Foundation grant IOS-1754884. Open Access funding provided by North Carolina State University. Deposited in PMC for immediate release.

Data availability

The raw data supporting the conclusions of this article are available on reasonable request from the authors.

References

Bishop, T., Lau, K. W., Epstein, A. C. R., Kim, S. K., Jiang, M., O'Rourke, D., Pugh, C. W., Gleadle, J. M., Taylor, M. S., Hodgkin, J. et al. (2004). Genetic

analysis of pathways regulated by the von Hippel-Lindau tumor suppressor in *Caenorhabditis elegans*. *PLoS Biol.* **2**, e289. doi:10.1371/journal.pbio.0020289

Blaszcak, J. R., Delesant, J. M., Urban, D. L., Doyle, M. W. and Bernhardt, E. S. (2019). Scoured or suffocated: Urban stream ecosystems oscillate between hydrologic and dissolved oxygen extremes. *Limnol. Oceanogr.* **64**, 877-894. doi:10.1002/lo.11081

Boutilier, R. G. and St-Pierre, J. (2000). Surviving hypoxia without really dying. *Comp. Biochem. Physiol. A. Mol. Integr. Physiol.* **126**, 481-490. doi:10.1016/S1095-6433(00)00234-8

Brodersen, K. P., Pedersen, O., Walker, I. R. and Jensen, M. T. (2008). Respiration of midges (Diptera; Chironomidae) in British Columbian lakes: O₂ regulation, temperature and their role as palaeo-indicators. *Freshw. Biol.* **53**, 593-602. doi:10.1111/j.1365-2427.2007.01922.x

Buchwalter, D., Scheibener, S., Chou, H., Soucek, D. and Elphick, J. (2019). Are sulfate effects in the mayfly *Neocloeon triangulifer* driven by the cost of ion regulation? *Philos. Trans. R. Soc. B Biol. Sci.* **374**, 20180013. doi:10.1098/rstb.2018.0013

Busch, K. E., Laurent, P., Soltesz, Z., Murphy, R. J., Faivre, O., Hedwig, B., Thomas, M., Smith, H. L. and De Bono, M. (2012). Tonic signaling from O₂ sensors sets neural circuit activity and behavioral state. *Nat. Neurosci.* **15**, 581-591. doi:10.1038/nn.3061

Chou, H., Pathmasiri, W., Deese-Spruill, J., Sumner, S. J., Jima, D. D., Funk, D. H., Jackson, J. K., Sweeney, B. W. and Buchwalter, D. B. (2018). The good, the bad, and the lethal: gene expression and metabolomics reveal physiological mechanisms underlying chronic thermal effects in mayfly larvae (*Neocloeon triangulifer*). *Front. Ecol. Evol.* **6**, 27. doi:10.3389/fevo.2018.00027

Cochran, J. K. and Buchwalter, D. B. (2022). The acclimatory response of the mayfly *Neocloeon triangulifer* to dilute conditions is linked to the plasticity of sodium transport. *Proc. R. Soc. B Biol. Sci.* **289**, 20220529. doi:10.1098/rspb.2022.0529

Cochran, J. K., Orr, S. E. and Buchwalter, D. B. (2021). Assessing the *P*_{crit} in relation to temperature and the expression of hypoxia associated genes in the mayfly, *Neocloeon triangulifer*. *Sci. Total Environ.* **808**, 151743. doi:10.1016/j.scitotenv.2021.151743

Cochran, J., Orr, S., Funk, D., Figurskey, A., Reiskind, M. and Buchwalter, D. (2024). Variation in freshwater insect osmoregulatory traits: a comparative approach. *Ecol. Evol. Physiol.* **97**, 164-179. doi:10.1086/730689

Conley, J. M., Watson, A. L. T. D., Xie, L. and Buchwalter, D. B. (2014). Dynamic selenium assimilation, distribution, efflux, and maternal transfer in Japanese medaka fed a diet of se-enriched mayflies. *Environ. Sci. Technol.* **48**, 2971-2978. doi:10.1021/es404933t

De Lima, T. M., Nery, L. E. M., Maciel, F. E., Ngo-Vu, H., Kozma, M. T. and Derby, C. D. (2021). Oxygen sensing in crustaceans: functions and mechanisms. *J. Comp. Physiol. A* **207**, 1-15. doi:10.1007/s00359-020-01457-z

Diaz, R. J. (2001). Overview of hypoxia around the world. *J. Environ. Qual.* **30**, 275-281. doi:10.2124/jeq2001.302275x

Epstein, A. C. R., Gleadle, J. M., McNeill, L. A., Hewitson, K. S., O'Rourke, J., Mole, D. R., Mukherji, M., Metzen, E., Wilson, M. I., Dhanda, A. et al. (2001). *C. elegans* EGL-9 and mammalian homologs define a family of dioxygenases that regulate HIF by prolyl hydroxylation. *Cell* **107**, 43-54. doi:10.1016/S0092-8674(01)00507-4

Eriksen, C. H. (1968). Ecological significance of respiration and substrate for burrowing Ephemeroptera. *Can. J. Zool.* **46**, 93-103. doi:10.1139/z68-015

Finbow, M. E. and Harrison, M. A. (1997). The vacuolar H⁺-ATPase: a universal proton pump of eukaryotes. *Biochem. J.* **324**, 697-712. doi:10.1042/bj3240697

Friedrich, J., Janssen, F., Aleynik, D., Bange, H. W., Boltacheva, N., Çagatay, M. N., Dale, A. W., Etiöpe, G., Erdem, Z., Geraga, M. et al. (2014). Investigating hypoxia in aquatic environments: diverse approaches to addressing a complex phenomenon. *Biogeosciences* **11**, 1215-1259. doi:10.5194/bg-11-1215-2014

Funk, D. H., Jackson, J. K. and Sweeney, B. W. (2006). Taxonomy and genetics of the parthenogenetic mayfly *Centroptilum triangulifer* and its sexual sister *Centroptilum alamance* (Ephemeroptera: Baetidae). *J. North Am. Benthol. Soc.* **25**, 417-429. doi:10.1899/0887-3593(2006)25[417:TAGOTP]2.0.CO;2

Funk, D. H., Sweeney, B. W. and Jackson, J. K. (2021). Oxygen limitation fails to explain upper chronic thermal limits and the temperature size rule in mayflies. *J. Exp. Biol.* **224**, jeb233388. doi:10.1242/jeb.233388

Giacomin, M., Onukwufor, J. O., Schulte, P. M. and Wood, C. M. (2020). Ionoregulatory aspects of the hypoxia-induced osmorespiratory compromise in the euryhaline Atlantic killifish (*Fundulus heteroclitus*): the effects of salinity. *J. Exp. Biol.* **223**, jeb216309. doi:10.1242/jeb.216309

Hawkins, C. P. (2006). Quantifying biological integrity by taxonomic completeness: its utility in regional and global assessments. *Ecol. Appl.* **16**, 1277-1294. doi:10.1890/1051-0761(2006)016[1277:QBIOTC]2.0.CO;2

Hawkins, C. P., Norris, R. H., Hogue, J. N. and Feminella, J. W. (2000). Development and evaluation of predictive models for measuring the biological integrity of streams. *Ecol. Appl.* **10**, 1456-1477. doi:10.1890/1051-0761(2000)010[1456:DAEOPM]2.0.CO;2

Hoback, W. W. and Stanley, D. W. (2001). Insects in hypoxia. *J. Insect Physiol.* **47**, 533-542. doi:10.1016/S0022-1910(00)00153-0

Hu, H., Boisson-Dernier, A., Israelsson-Nordström, M., Böhmer, M., Xue, S., Ries, A., Godoski, J., Kuhn, J. M. and Schroeder, J. I. (2010). Carbonic anhydrases are upstream regulators of CO₂-controlled stomatal movements in guard cells. *Nat. Cell Biol.* **12**, 87-93. doi:10.1038/ncb2009

Huryn, A. D. and Wallace, J. B. (2000). Life history and production of stream insects. *Annu. Rev. Entomol.* **45**, 83-110. doi:10.1146/annurev.ento.45.1.83

Iftikar, F. I., Matey, V. and Wood, C. M. (2010). The ionoregulatory responses to hypoxia in the freshwater rainbow trout *Oncorhynchus mykiss*. *Physiol. Biochem. Zool.* **83**, 343-355. doi:10.1086/648566

Jenny, J.-P., Francus, P., Normandeau, A., Lapointe, F., Perga, M.-E., Ojala, A., Schimmelmann, A. and Zolitschka, B. (2016a). Global spread of hypoxia in freshwater ecosystems during the last three centuries is caused by rising local human pressure. *Glob. Change Biol.* **22**, 1481-1489. doi:10.1111/gcb.13193

Jenny, J.-P., Normandeau, A., Francus, P., Tararu, Z. E., Gregory-Eaves, I., Lapointe, F., Jautz, J., Ojala, A. E. K., Dorioz, J.-M., Schimmelmann, A. et al. (2016b). Urban point sources of nutrients were the leading cause for the historical spread of hypoxia across European lakes. *Proc. Natl. Acad. Sci.* **113**, 12655-12660. doi:10.1073/pnas.1605480113

Johnson, B. R., Weaver, P. C., Nietch, C. T., Lazorchak, J. M., Struewing, K. A. and Funk, D. H. (2015). Elevated major ion concentrations inhibit larval mayfly growth and development. *Environ. Toxicol. Chem.* **34**, 167-172. doi:10.1002/etc.2777

Jonusaitė, S., Kelly, S. P. and Donini, A. (2013). Tissue-specific ionomotive enzyme activity and K⁺ reabsorption reveal the rectum as an important ionoregulatory organ in larval *Chironomus riparius* exposed to varying salinity. *J. Exp. Biol.* **216**, 3637-3648. doi:10.1242/jeb.089219

Keil, T. A. (2012). Sensory cilia in arthropods. *Arthropod. Struct. Dev.* **41**, 515-534. doi:10.1016/j.asd.2012.07.001

Kim, K. S., Chou, H., Funk, D. H., Jackson, J. K., Sweeney, B. W. and Buchwalter, D. B. (2017). Physiological responses to short-term thermal stress in mayfly (*Neocloeon triangulifer*) larvae in relation to upper thermal limits. *J. Exp. Biol.* **220**, 2598-2605. doi:10.1242/jeb.156919

Kunz, J. L., Conley, J. M., Buchwalter, D. B., Norberg-King, T. J., Kemble, N. E., Wang, N. and Ingersoll, C. G. (2013). Use of reconstituted waters to evaluate effects of elevated major ions associated with mountaintop coal mining on freshwater invertebrates. *Environ. Toxicol. Chem.* **32**, 2826-2835. doi:10.1002/etc.2391

Lencioni, V., Bernabò, P., Vanin, S., Di Muro, P. and Beltramini, M. (2008). Respiration rate and oxy-regulatory capacity in cold stenothermal chironomids. *J. Insect Physiol.* **54**, 1337-1342. doi:10.1016/j.jinsphys.2008.07.002

Ma, D. K. and Ringstad, N. (2012). The neurobiology of sensing respiratory gases for the control of animal behavior. *Front. Biol.* **7**, 246-253. doi:10.1007/s11515-012-1219-x

Markovich, D. and Aronson, P. S. (2007). Specificity and regulation of renal sulfate transporters. *Annu. Rev. Physiol.* **69**, 361-375. doi:10.1146/annurev.physiol.69.040705.141319

Meire, L., Soetaert, K. E. R. and Meysman, F. J. R. (2013). Impact of global change on coastal oxygen dynamics and risk of hypoxia. *Biogeosciences* **10**, 2633-2653. doi:10.5194/bg-10-2633-2013

Nixon, S. W. (1995). Coastal marine eutrophication: a definition, social causes, and future concerns. *Ophelia* **41**, 199-219. doi:10.1080/00785236.1995.10422044

Nowghani, F., Jonusaitė, S., Watson-Leung, T., Donini, A. and Kelly, S. P. (2017). Strategies of ionoregulation in the freshwater nymph of the mayfly *Hexagenia rigida*. *J. Exp. Biol.* **220**, 3997-4006. doi:10.1242/jeb.166132

O'Leary, N. A., Wright, M. W., Brister, J. R., Ciuffo, S., Haddad, D., McVeigh, R., Rajput, B., Robbertse, B., Smith-White, B., Ako-Adjei, D. et al. (2016). Reference sequence (RefSeq) database at NCBI: current status, taxonomic expansion, and functional annotation. *Nucleic Acids Res.* **44**, D733-D745. doi:10.1093/nar/gkv1189

Onukwufor, J. O. and Wood, C. M. (2018). The osmorespiratory compromise in rainbow trout (*Oncorhynchus mykiss*): the effects of fish size, hypoxia, temperature and strenuous exercise on gill diffusive water fluxes and sodium net loss rates. *Comp. Biochem. Physiol. A Mol. Integr. Physiol.* **219**, 10-18. doi:10.1016/j.cbpa.2018.02.002

Onukwufor, J. O. and Wood, C. M. (2020). Osmorespiratory compromise in Zebrafish (*Danio rerio*): effects of hypoxia and acute thermal stress on oxygen consumption, diffusive water flux, and sodium net loss rates. *Zebrafish* **17**, 400-411. doi:10.1089/zeb.2020.1947

Orr, S. E., Negrão Watanabe, T. T. and Buchwalter, D. B. (2021). Physiological plasticity and acclimatory responses to salinity stress are ion-specific in the mayfly, *Neocloeon triangulifer*. *Environ. Pollut.* **286**, 117221. doi:10.1016/j.envpol.2021.117221

Orr, S. E., Collins, L. B., Jima, D. D. and Buchwalter, D. B. (2023). Salinity-induced ionoregulatory changes in the gill proteome of the mayfly, *Neocloeon triangulifer*. *Environ. Pollut.* **316**, 120609. doi:10.1016/j.envpol.2022.120609

Piaff, M. W. (2001). A new mathematical model for relative quantification in real-time RT-PCR. *Nucleic Acids Res.* **29**, e45. doi:10.1093/nar/29.9.e45

Pörtner, H.-O. and Grieshaber, M. (1993). Critical PO₂ (s) in oxyconforming and oxyregulating animals gas exchange, metabolic rate and the mode of energy production. In *The Vertebrate Gas Transport Cascade Adaptations to*

Environment and Mode of Life (ed. J. E. P. W. Bicudo), pp. 330-357. Boca Raton, FL: CRC Press.

Rebora, M., Salerno, G. and Piersanti, S. (2019). Aquatic insect sensilla: morphology and function. *Aquat. Insects Behav. Ecol.* **91**, 139-166. doi:10.1007/978-3-030-16327-3_7

Resh, V. H. and Jackson, J. K. (1993). Rapid assessment approaches to biomonitoring using benthic macroinvertebrates. In *Freshwater Biomonitoring and Benthic Macroinvertebrates* (ed. D. Rosenberg, M. Resh and H. Vincent), pp. 195-233. New York: Chapman & Hall.

Resh, V. H., Lamberti, G. A., Buchwalter, D. and Eriksen, C. H. (2008). Aquatic insect respiration. In *An Introduction to the Aquatic Insects of North America* (ed. R. W. Merritt and K. W. Cummins), pp. 39-54. Kendall/Hunt Publishing Co.

Robertson, L. M., Val, A. L., Almeida-Val, V. F. and Wood, C. M. (2015). Ionoregulatory aspects of the osmorespiratory compromise during acute environmental hypoxia in 12 tropical and temperate teleosts. *Physiol. Biochem. Zool.* **88**, 357-370. doi:10.1086/681265

Scheibener, S. A., Richardi, V. S. and Buchwalter, D. B. (2016). Comparative sodium transport patterns provide clues for understanding salinity and metal responses in aquatic insects. *Aquat. Toxicol.* **171**, 20-29. doi:10.1016/j.aquatox.2015.12.006

Scott, K. (2011). Out of thin air: sensory detection of oxygen and carbon dioxide. *Neuron* **69**, 194-202. doi:10.1016/j.neuron.2010.12.018

Semenza, G. L. (2001). HIF-1, O₂, and the 3 PHDs: how animal cells signal hypoxia to the nucleus. *Cell* **107**, 1-3. doi:10.1016/S0092-8674(01)00518-9

Shao, Z., Zhang, Y. and Powell-Coffman, J. A. (2009). Two distinct roles for EGL-9 in the regulation of HIF-1-mediated gene expression in *Caenorhabditis elegans*. *Genetics* **183**, 821-829. doi:10.1534/genetics.109.107284

Shen, C. and Powell-Coffman, J. A. (2003). Genetic analysis of hypoxia signaling and response in *C. elegans*. *Ann. N. Y. Acad. Sci.* **995**, 191-199. doi:10.1111/j.1749-6632.2003.tb03222.x

Silver, S. and Donini, A. (2021). Physiological responses of freshwater insects to salinity: molecular-, cellular- and organ-level studies. *J. Exp. Biol.* **224**, jeb222190. doi:10.1242/jeb.222190

Soucek, D. J. and Dickinson, A. (2015). Full-life chronic toxicity of sodium salts to the mayfly *Neocloeon triangulifer* in tests with laboratory cultured food. *Environ. Toxicol. Chem.* **34**, 2126-2137. doi:10.1002/etc.3038

Sweeney, B. W. and Vannote, R. L. (1984). Influence of food quality and temperature on life-history characteristics of the parthenogenetic mayfly, *Cloeon triangulifer*. *Freshw. Biol.* **14**, 621-630. doi:10.1111/j.1365-2427.1984.tb00181.x

Sweeney, B. W., Funk, D. H. and Standley, L. J. (1993). Use of the stream mayfly *cloeon-triangulifer* as a bioassay organism - life-history response and body burden following exposure to technical chlordane. *Environ. Toxicol. Chem.* **12**, 115-125. doi:10.1002/etc.5620120113

Tashian, R. E. (1989). The carbonic anhydrases: widening perspectives on their evolution, expression and function. *BioEssays* **10**, 186-192. doi:10.1002/bies.950100603

Verberk, W. C. E. P., Buchwalter, D. B. and Kefford, B. J. (2020). Energetics as a lens to understanding aquatic insect's responses to changing temperature, dissolved oxygen and salinity regimes. *Curr. Opin. Insect Sci.* **41**, 46-53. doi:10.1016/j.cois.2020.06.001

Weihrauch, D., Ziegler, A., Siebers, D. and Towle, D. W. (2001). Molecular characterization of V-type H⁺-ATPase (B-subunit) in gills of euryhaline crabs and its physiological role in osmoregulatory ion uptake. *J. Exp. Biol.* **204**, 25-37. doi:10.1242/jeb.204.1.25

Wichard, W., Tsui, P. T. P. and Komnick, H. (1973). Effect of different salinities on the coniform chloride cells of mayfly larvae. *J. Insect Physiol.* **19**, 1825-1835. doi:10.1016/0022-1910(73)90051-6

Wood, C. M. (2018). The fallacy of the P_{crit} – are there more useful alternatives? *J. Exp. Biol.* **221**, jeb163717. doi:10.1242/jeb.163717

Wood, C. M. and Eom, J. (2021). The osmorespiratory compromise in the fish gill. *Comp. Biochem. Physiol. A Mol. Integr. Physiol.* **254**, 110895. doi:10.1016/j.cbpa.2021.110895

Wood, C. M., Kajimura, M., Sloman, K. A., Scott, G. R., Walsh, P. J., Almeida-Val, V. M. F. and Val, A. L. (2007). Rapid regulation of Na⁺ fluxes and ammonia excretion in response to acute environmental hypoxia in the Amazonian oscar, *Astronotus ocellatus*. *Am. J. Physiol.-Regul. Integr. Comp. Physiol.* **292**, R2048-R2058. doi:10.1152/ajpregu.00640.2006

Wood, C. M., Iftikar, F. I., Scott, G. R., De Boeck, G., Sloman, K. A., Matey, V., Valdez Domingos, F. X., Duarte, R. M., Almeida-Val, V. M. F. and Val, A. L. (2009). Regulation of gill transcellular permeability and renal function during acute hypoxia in the Amazonian oscar (*Astronotus ocellatus*): new angles to the osmorespiratory compromise. *J. Exp. Biol.* **212**, 1949-1964. doi:10.1242/jeb.028464

Wood, C. M., Ruhr, I. M., Schauer, K. L., Wang, Y., Mager, E. M., McDonald, M. D., Stanton, B. and Grosell, M. (2019). The osmorespiratory compromise in the euryhaline killifish: water regulation during hypoxia. *J. Exp. Biol.* **222**, jeb204818. doi:10.1242/jeb.204818

Xie, L. and Buchwalter, D. B. (2011). Cadmium exposure route affects antioxidant responses in the mayfly *Centroptilum triangulifer*. *Aquat. Toxicol.* **105**, 199-205. doi:10.1016/j.aquatox.2011.06.009